

RNase-L regulates the stability of mitochondrial DNA-encoded mRNAs in mouse embryo fibroblasts

Krish Chandrasekaran^{a,*}, Zara Mehrabian^a, Xiao-Ling Li^b, Bret Hassel^b

^a Department of Anesthesiology, University of Maryland School of Medicine, Baltimore, MD 21201, USA

^b Greenbaum Cancer Center, University of Maryland School of Medicine, Baltimore, MD 21201, USA

Received 29 September 2004

Available online 22 October 2004

Abstract

Accelerated decrease in the levels of mitochondrial DNA-encoded mRNA (mt-mRNA) occurs in neuronal cells exposed either to the excitatory amino acid, glutamate or to the sodium ionophore, monensin, suggesting a role of mitochondrial RNase(s) on the stability of mt-mRNAs. Here we report that in mouse embryo fibroblasts that are devoid of the interferon-regulated RNase, RNase-L, the monensin-induced decrease in the half-life of mt-mRNA was reduced. In monensin (250 nM)-treated RNase-L^{+/+} cells the average half-life of mt-mRNA, determined after termination of transcription with actinomycin D, was found to be 3 h, whereas in monensin-treated RNase-L^{-/-} cells the half-life of mt-mRNA was >6 h. In contrast, the stability of nuclear DNA-encoded β -actin mRNA was unaffected. Induction of RNase-L expression in mouse 3T3 fibroblasts further decreased the monensin-induced reduction in mt-mRNA half-life to 1.5 h. The results indicate that the RNase-L-dependent decrease in mtDNA-encoded mRNA transcript levels occurs through a decrease in the half-life of mt-mRNA, and that RNase-L may play a role in the stability of mt-mRNA.

© 2004 Elsevier Inc. All rights reserved.

Keywords: Monensin; Glutamate; Signal transducers and activators of transcription 1; Mitochondrial DNA; Transcription; Post-transcription; mRNA stability; Interferon; Interferon regulatory factor 1; Ischemia; RNase-L; RNase

Mitochondrial oxidative phosphorylation system (OXPHOS) consists of five multi-subunit enzyme complexes and is responsible for the generation of ATP [1]. Four of these OXPHOS complexes are bipartite in nature consisting of subunits derived from both mitochondrial DNA (mtDNA) and nuclear DNA (nDNA) [1,2]. Mitochondrial DNA encodes 13 polypeptides, all of which are necessary for electron transport and oxidative phosphorylation [1,2]. The large number of remaining subunits is specified by the nuclear genome [1]. To form active enzyme complexes, both mtDNA and nDNA-encoded subunits are required [1]. Mitochondrial gene products are thus essential for the regulation

of energy metabolism in the cell; accordingly, mitochondrial (mt) gene expression is responsive to changes in cellular energy demand [3–5]. For example, high mitochondrial ATP levels reflect a low cellular energy demand and lead to a reduced transcription of mtDNA [6–8]. In contrast to this transcriptional regulation, our recent studies identified a post-transcriptional, energy state-independent response in which mt gene expression is down-regulated in conditions of mitochondrial stress [9]. Specifically, treatment of PC12 cells with the sodium ionophore, monensin, increased cellular energy consumption, but decreased the steady-state levels of mt-RNAs by 50% within 3–4 h [9]. Determination of the half-lives ($t_{1/2}$) of mtDNA-encoded mRNAs and 12S rRNA, and nuclear-encoded β -actin mRNA revealed a selective decrease in $t_{1/2}$ from 3.5 to 1 h, whereas the $t_{1/2}$ of 12S rRNA and β -actin mRNA was unchanged

* Corresponding author. Fax: +1 410 706 2550.

E-mail address: kchandra@anesthlab.umm.edu (K. Chandrasekaran).

over 24 h [9]. These results indicated the existence of a mechanism to modulate mt-mRNA stability in response to cell stress.

The control of mRNA stability is an important mechanism to regulate gene expression [10–13]. The *cis*-acting RNA determinants and the *trans*-acting RNA binding proteins have been identified for numerous labile mRNAs; however, the specific ribonucleases involved, and mechanistic details of RNA decay, remain to be determined [11–13]. Little is known about the post-transcriptional regulation of mt-mRNAs [14]; indeed, these mt-mRNAs lack two of the best characterized determinants of mRNA stability that are found in nuclear-encoded mRNAs, namely a long 3' poly(A) tract and a 5' CAP structure [15–18]. Recently, an interferon-regulated ribonuclease, RNase-L, was implicated in the degradation of mt-RNAs in response to interferon (IFN) treatment [19]. Furthermore, this down-regulation of mt-mRNAs correlated with sensitivity to the antiproliferative activity of IFN [19,20]. RNase-L exists in a latent state in cells; its allosteric activator, 2–5A [(pp)p5'A2'(p5'A2')_n, $n \geq 2$], is produced by a family of 2–5A synthetase enzymes in reactions requiring double-stranded RNA [21,22]. 2–5A binding results in the dimerization and activation of RNase-L [23]. A role for RNase-L in antiviral, pro-apoptotic, and growth inhibitory activities has been established; however, the relevant RNA substrates of RNase-L have not been identified [24–28].

In this study, we investigated the hypothesis that RNase-L regulates mitochondrial gene expression by its effect on the stability of mt-mRNA in cells subjected to chronic exposure to the sodium ionophore, monensin. We measured the stability and the steady state levels of mt-mRNAs and control β -actin mRNA in monensin-treated mouse embryo fibroblasts (MEF) that contain RNase-L (RNase-L^{+/+}), or are devoid of RNase-L (RNase-L^{-/-}), and in murine 3T3 cells that were transfected with inducible RNase-L. Our results indicate that in monensin-treated cells the half-lives of mt-mRNAs were increased in RNase-L^{-/-} cells compared to RNase-L^{+/+} cells and the half-lives of mt-mRNAs were decreased in RNase-L-induced cells, suggesting a role for RNase-L in regulating mt-mRNA stability in response to cellular ionic stress.

Materials and methods

Cell cultures. Cell cultures were maintained in a humidified atmosphere of 5% CO₂, 95% balanced air at 37 °C. Cells were cultured in the following growth media: RNase-L^{+/+} and ^{-/-} mouse embryo fibroblasts ([29]; generously supplied by Robert H. Silverman, The Cleveland Clinic Foundation) were maintained in Dulbecco's modified Eagle's medium (DMEM) with 10% fetal calf serum and 1% antibiotic/antimycotic. Construction of inducible RNase-L-stable transfectants into NIH 3T3 cells has been described [24]. 3T3 cells were maintained

in DMEM with 10% fetal calf serum, 1% antibiotic/antimycotic, 50 μ g/ml hygromycin, and 500 μ g/ml G418. Expression of RNase-L was induced by the addition of 3 mM isopropyl β -D-thiogalactopyranoside (IPTG) for a period of 48 h. Cell viability was measured by trypan blue exclusion.

Reagents. All reagents and chemicals used were of the highest grade available from Sigma Chemical (St. Louis, MS, USA). Stock solution of actinomycin D was prepared in water, whereas monensin was dissolved in 95% ethanol. When ethanol was used as a solvent, appropriate control experiments were conducted using the solvent alone. Ethanol concentrations were always <0.1%.

Experimental procedure. Cells were grown in 60 \times 15 mm dishes. Monensin (250 nM) was added to the culture medium. At defined timed periods, cells were washed with Dulbecco's phosphate-buffered saline (DPBS) without calcium and magnesium, and total RNA was isolated using RNA-Bee reagent as recommended by the manufacturer (TEL-TEST, TX). Total RNA was subjected to Northern blot analysis as described below. The stability of mtDNA- and nDNA-encoded transcripts was determined by adding the transcriptional inhibitor actinomycin D to the cultures at a final concentration of 5 μ g/ml. The cells were incubated for 30 min. Monensin was then added to the culture medium. Total RNA was isolated at various times over a 6-h period and processed for RNA analysis.

RNA analysis. Two to ten micrograms of total RNA was run on a 1.2% formaldehyde agarose gel, stained with ethidium bromide, 28S and 18S rRNA were imaged and quantified to confirm equal loading of RNA. The gel was then transferred onto a GeneScreen Plus membrane (Dupont, New England Nuclear, MA, USA). Prehybridization and hybridization were done with Hybridizol reagent (Hybridizol I and II mixed in the ratio of 3:2, Serologicals, GA, USA). The blots were prehybridized at 37 °C for 16 h and hybridized with ³²P-labeled mtDNA- and nDNA-encoded gene probes at 37 °C for 48 h [30]. The blots were washed with increasing stringency and the final wash was performed at 65 °C with 0.2 \times SSC (1 \times SSC = 150 mM sodium chloride and 15 mM sodium citrate) and 1% SDS (sodium dodecyl sulfate). The blots were exposed to X-ray film (Bio-max MR, Kodak, NY, USA) with an intensifying screen for 45 min to 2 days at -70 °C. Probe was removed from the blots by placing them in boiling DEPC-treated water for 10 min. The blots were then rehybridized with a ³²P-labeled control β -actin probe as described above. The level of RNA hybridized was quantified using an image analysis program. To maintain measured intensities within the linear range, the blots hybridized with different probes were exposed for different periods of time. The level of RNA was quantified by densitometry from autoradiograms of lower exposure than was used for photography. Ratios of mt-mRNA to β -actin mRNA were calculated as described previously [30].

Probe preparation and labeling. An mtDNA probe that detects simultaneously several mt-mRNAs was used. The probe was created by amplification of nucleotides (nt) 8861–14549 of mtDNA. This probe hybridizes to ND5, ND4&4L, cytochrome *b*, and COX III mRNAs. A cDNA insert of β -actin cDNA clone was used as probe. The probes were radiolabeled by the random primer method and hybridized to the blots.

Estimation of half-lives of mt-mRNAs and β -actin mRNA. Two micrograms of total RNA from cells treated with monensin in the presence of actinomycin D was subjected to Northern blot analysis. The blots were hybridized with mtDNA and β -actin probes as described and the levels of respective RNA species were quantified. Levels of mt-mRNA were calculated as the ratio of the respective species to the level of β -actin mRNA. At each experimental time, the RNA ratios are expressed as a percentage of the ratio at time zero. The half-lives were determined from the equation $t_{1/2} = 0.301/\text{slope}$ of the best-fit line (\log_{10} remaining RNA versus time) [9].

Statistical analysis. The results presented are representative of at least three independent experiments. Statistical analysis was carried out using a one-way analysis of variance (ANOVA) followed by Tukey's test for multiple comparisons. Means \pm SEM are presented. Differences were considered significant when $P < 0.05$.

Results and discussion

Transient exposure of primary neurons to glutamate or chronic exposure of PC12S cells to the sodium ionophore, monensin, decreased the half-lives ($t_{1/2}$) of mtDNA-encoded mRNAs from 3.5 to 1 h, whereas the $t_{1/2}$ of mtDNA-encoded 12S rRNA and nDNA-encoded β -actin mRNA were unchanged from 24 h [9]. These results indicated the existence of a mechanism to modulate mt-mRNA stability in response to cell stress. Recently, it has been shown that RNase-L activity regulates the stability of mitochondrial mRNA (mt-mRNA) in interferon treated human H9 cells [19]. To determine whether the presence or absence of RNase-L would alter the stability and thereby the steady-state levels of mt-mRNA under conditions of chronic exposure to monensin, embryonic fibroblasts from wild type (WT) mice (RNase-L^{+/+}) and from mice that are devoid of RNase-L (RNase-L^{-/-}) were employed. RNase-L^{-/-} mice were generated by the insertion of *neomycin* gene in codon number 100 in the first exon of the RNase-L gene [29]. To confirm the presence and absence of *neo* insertion within RNase-L gene in the RNase-L^{-/-} and RNase-L^{+/+} mouse embryo fibroblasts, respectively, genomic DNA was prepared from these cells and a polymerase chain reaction using RNase-L specific primers [5'-ACCATGGAGACCCCGGATTAT-3' (nt 161–181) and 5'-GTCCTTCGTTGTCTGTCGTCG-3' (nt 643–623)] was carried out. The result is shown in Fig. 1A. The presence of RNase-L in RNase-L^{+/+} gave a 500 bp DNA PCR fragment, whereas the absence of RNase-L in RNase-L^{-/-} gave a 1600 bp DNA *neo* containing PCR fragment.

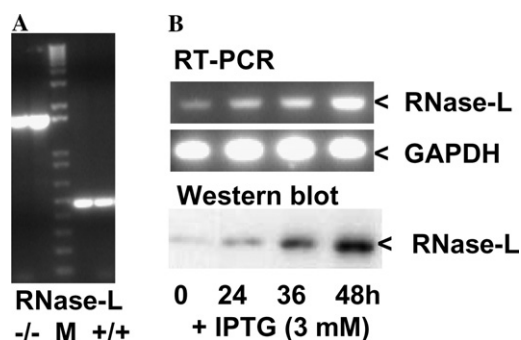


Fig. 1. Characterization and induction of RNase-L in mouse embryo fibroblasts. (A) Genomic DNA was isolated from RNase-L^{+/+} and RNase-L^{-/-} mouse embryo fibroblasts and subjected to PCR using RNase-L-specific primers. Insertion of the *neo* gene in the RNase-L gene first exon was confirmed by the presence of a 1600 bp DNA *neo* containing PCR fragment and by the absence of a 500 bp DNA PCR fragment of the wild type. (B) RNase-L was induced by the addition of the inducer IPTG (3 mM) to the culture medium. At the indicated time periods total RNA or protein was isolated. The RNA samples were subjected to RT-PCR. The protein samples were subjected to Western blot analysis using RNase-L specific antibody.

The stability of mitochondrial mRNA is increased in the absence of RNase-L in monensin-treated cells

To examine the effects of monensin on mt-mRNA expression in RNase-L^{+/+} and RNase-L^{-/-} cells, monensin (250 nM) was added to the culture medium. At timed intervals over a 6-h period total cellular RNA was isolated and subjected to Northern blot analysis. Blots were stained with methylene blue to confirm equal loadings and transfer between lanes. Blots were probed with an mtDNA probe that hybridizes to four mtDNA-encoded mRNAs (ND5, ND4&4L, cytochrome *b*, and COX III) and relative levels were quantified by densitometry. The results are shown in Fig. 2A. Exposure of RNase-L^{+/+} cells to monensin caused a significant decrease in the levels of mRNA species derived from both the light and heavy strand, of mtDNA at 2–6 h. This was preceded by an increase in the levels of mt-mRNAs during the first hour of monensin treatment. In contrast, no significant decreases in the levels of mt-mRNAs were seen in monensin-treated RNase-L^{-/-} cells (Fig. 2A). The levels of control transcript, nDNA-encoded β -actin mRNA, showed no significant changes in monensin-treated RNase-L^{+/+} and ^{-/-} cells. Calculation of the ratio of mt-mRNA to β -actin mRNA revealed that the ratio was significantly different in monensin-treated RNase-L^{+/+} cells at 2–6 h time points compared to 0 time. Thus, the steady state levels of mt-mRNA were higher in monensin-treated RNase-L^{-/-} cells compared to RNase-L^{+/+} cells.

To determine if the increase in the steady state levels of mt-mRNA in monensin-treated RNase-L^{-/-} cells is due to an increase in the stability of these transcripts, we measured the half-life of mt-mRNA. Actinomycin D was added to the culture medium of RNase-L^{+/+} and RNase-L^{-/-} cells, monensin (250 nM) was then added to the culture medium. Total RNA was isolated at time points over a 6-h-treatment period. The yield of total RNA decreased slightly after inhibition of transcription; however, cell viability was not compromised by this treatment. Levels of mt-mRNAs were analyzed by Northern blot and quantified by densitometry (Fig. 2B). Significantly higher levels of mt-mRNAs were observed in actinomycin-monensin-treated RNase-L^{-/-} cells compared to RNase-L^{+/+} cells and the mt-mRNAs were found to be significantly stabilized in RNase-L^{-/-} cells (Fig. 2B). The mt-mRNA half-lives, determined after termination of transcription with actinomycin D, increased from 3 h in RNase-L^{+/+} cells to >6 h in RNase-L^{-/-} cells (Fig. 2B).

Induction of RNase-L decreases the stability of mt-mRNA

To assess the implication that RNase-L may regulate the stability of mt-mRNA, an IPTG-inducible

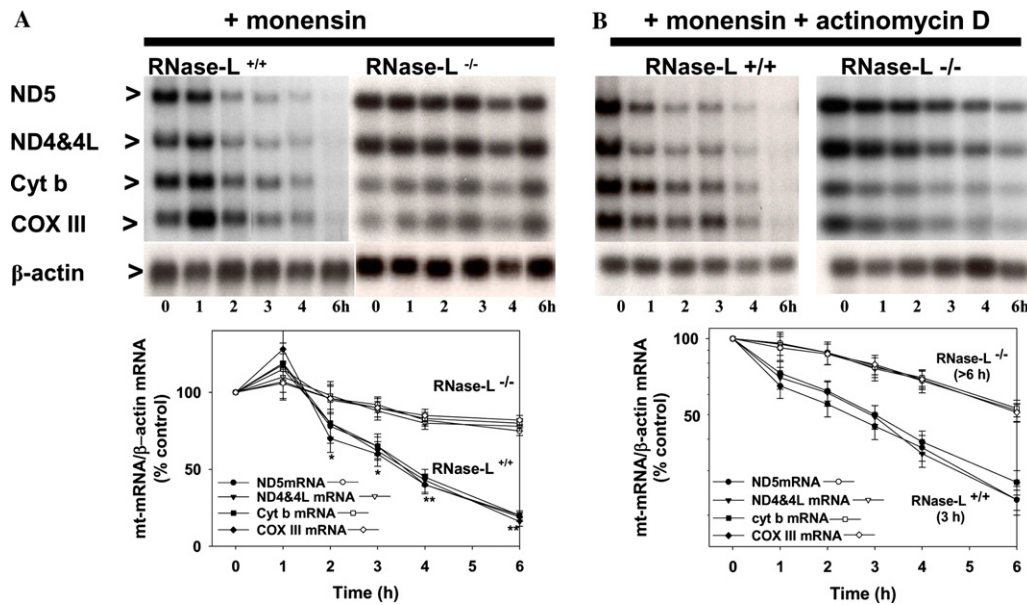


Fig. 2. Mitochondrial transcripts are stabilized in monensin-treated RNase-L^{-/-} cells. (A) RNase-L^{+/+} and RNase-L^{-/-} mouse embryo fibroblasts were exposed to monensin (final concentration 250 nM) for the indicated time periods. Two microgram aliquots of total RNA were subjected to Northern blot analysis. The intensity of the hybridization signal was quantified by image analysis of the autoradiograms. The ratio of individual mtDNA-encoded mRNA to β-actin mRNA was calculated at each time point. The percentage of RNA change compared to those of zero time samples are shown. Data points are the mean of three independent experiments. Standard error bars of means are shown. * indicates significant from zero time samples ($P < 0.05$), ** indicates significant from zero time samples ($P < 0.01$). Note significant decreases were observed only in monensin-treated RNase-L^{+/+} cells. (B) RNase-L^{+/+} and RNase-L^{-/-} mouse embryo fibroblasts were exposed to monensin (final concentration 250 nM) and actinomycin D (5 μg/ml) for the indicated time periods. Total RNA was isolated and 2 μg aliquots were subjected to Northern blot analysis. The intensity of the hybridization signal was quantified by image analysis of the autoradiograms. The ratio of individual mtDNA-encoded mRNA to β-actin mRNA was calculated at each time point. Semi-log plots of the percentage of RNA change compared to that of zero time sample is shown. The half-lives were determined from the equation $t_{1/2} = 0.301/\text{slope of the best fit line (log}_{10} \text{ remaining RNA versus time)}$.

RNase-L gene was introduced into mouse NIH 3T3 cells. Expression of RNase-L was induced with IPTG (3 mM) for 48 h. The induction of RNase-L was confirmed by RT-PCR and by Western blot analysis (Fig. 1B). Uninduced and RNase-L-induced cells were then exposed to monensin (250 nM) in the culture medium. The RNA samples were subjected to Northern blot analysis. The stability of mt-mRNA was determined in cells before and after induction of expression of RNase-L by the addition of monensin and actinomycin D to the culture medium. The Northern blot results are shown in Fig. 3A and the semi-log plot of the half-life in Fig. 3B. Clearly significantly higher levels of mt-mRNAs were present in non-induced cells compared to RNase-L-induced cells (Fig. 3A) and the mt-mRNAs were significantly destabilized in RNase-L induced cells (Fig. 3B), decreasing the estimated half-life of mt-mRNA from 4 to 1.5 h.

The results of the present study demonstrate that presence of RNase-L caused a significant decrease in the steady state mtDNA-encoded mRNA level in mouse embryo fibroblasts exposed chronically to the sodium ionophore, monensin. The levels of mtDNA-encoded ND5, ND4&4L, cytochrome *b*, and COX III mRNAs were decreased in monensin-treated RNase-L^{+/+} cells compared to RNase-L^{-/-} cells. Estimation of mtDNA

by dot blot analysis showed no significant differences in mtDNA levels between RNase-L^{+/+} and ^{-/-} cells (not shown). The observed decrease in mt-mRNA levels in monensin-treated RNase-L^{+/+} cells appears to be not due to either loss of mitochondria or a general breakdown of RNA. On the other hand, hybridization with another mtDNA probe (nt 3351–7570) that recognizes mtDNA-encoded ND1, ND2, COX I, and COX II mRNAs showed a similar reduction in mt-mRNA in monensin-treated RNase-L^{+/+} cells (not shown). Thus, the effect of RNase-L appears to be not specific for any one particular mt-mRNA. This may relate to the similarity in the stability of all mtDNA-encoded mRNAs. Mitochondrial mRNA species are found to be metabolically unstable, with half-lives of 2.5–3.5 h in HeLa cells [31]. The estimated half-lives of mt-mRNA (~3 h) observed in mouse fibroblasts in this study are similar to the results reported in other cell culture systems. However, the RNase(s) that may be responsible for the short half-life of mt-mRNA have not been identified. The steady-state levels of mt-mRNA were higher in RNase-L^{-/-} cells compared to RNase-L^{+/+} cells and induction of RNase-L in the 3T3 cells showed a decrease in the steady-state levels of mt-mRNA (also at 0 time in Fig. 3). Based on the results presented here together with the reported localization of RNase-L to mitochondria

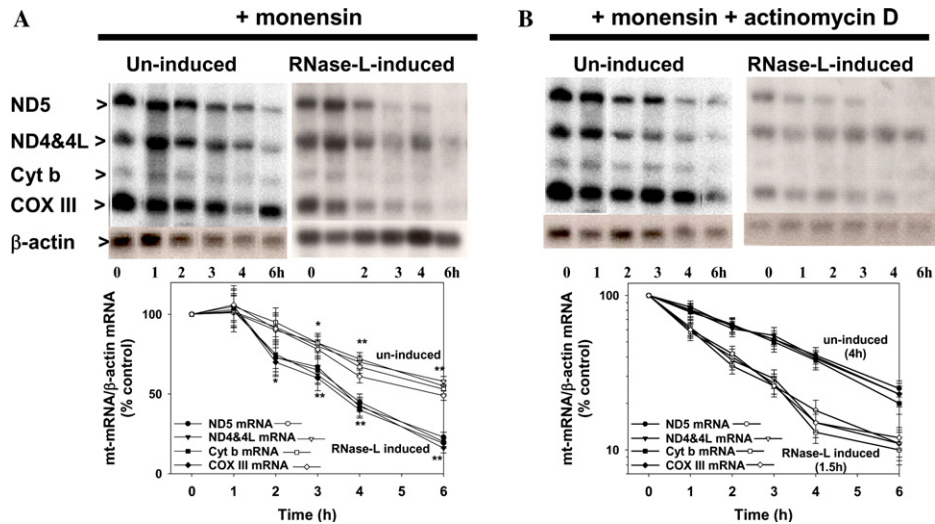


Fig. 3. Mitochondrial transcripts are de-stabilized in RNase-L-induced 3T3 cells. $n = 3$. (A) RNase-L was induced by the addition of IPTG (3 mM) to the culture medium for 48 h. Uninduced and RNase-L-induced 3T3 cells were then exposed to monensin (final concentration 250 nM) for the indicated time periods. Two microgram aliquots of total RNA were subjected to Northern blot analysis. The intensity of the hybridization signal was quantified by image analysis of the autoradiograms. The ratio of individual mtDNA-encoded mRNA to β -actin mRNA was calculated at each time point. The percentage of RNA change compared to those of zero time samples are shown. * indicates significant from zero time samples ($P < 0.05$), ** indicates significant from zero time samples ($P < 0.01$). Data points are the mean of three independent experiments. Standard error bars of means are shown. (B) Uninduced and RNase-L-induced 3T3 cells were exposed to monensin (final concentration 250 nM) and actinomycin D (5 μ g/ml) for the indicated time periods. Total RNA was isolated and 2 μ g aliquots were subjected to Northern blot analysis. The intensity of the hybridization signal was quantified by image analysis of the autoradiograms. The ratio of individual mtDNA-encoded mRNA to β -actin mRNA was calculated at each time point. Semi-log plots of the percentage of RNA change compared to that of zero time sample is shown. The half-lives were determined from the equation $t_{1/2} = 0.301/\text{slope of the best fit line (log}_{10} \text{ remaining RNA versus time)}$.

[19] it is likely that RNase-L is also responsible for the normal turnover of mt-mRNA.

A previous study showed that addition of interferon α decreases the stability of mt-mRNA by regulating RNase-L expression. The result of this study showed that the stability of mt-mRNA was decreased by RNase-L in the absence of IFN treatment in cells exposed to monensin. Interferon activates RNase-L pathway by a mechanism that involves the synthesis of an allosteric activator, 2-5A, from ATP by a family of 2-5A synthetase enzymes [oligo adenylate synthetase (OAS)] in reactions requiring double-stranded (ds) RNA [21,22,32]. Binding of 2-5A to RNase-L results in the dimerization and activation of RNase-L [23]. OAS and RNase-L are constitutively expressed at low basal levels and localized predominantly to the cytosol [33,34]. Ultrastructural localization in a human lymphoid cell line that overexpresses OAS showed that OAS is also localized to mitochondria [34] and recently RNase-L was also reported to be localized to mitochondria in HeLa cells [19]. In addition, presence of double-stranded RNA, due to the bidirectional transcription of mtDNA, has been observed in HeLa cell mitochondria [35]. Thus, with mitochondria being the site of ATP synthesis, a potential for activation of RNase-L pathway by dsRNA exists particularly in cells subjected to sudden energy demand by the addition of the sodium ionophore, monensin. This is consistent with the observa-

tions which suggest that cellular stress responses induced by IFN in response to viral infections are also activated in ischemic injury. Neuronal activation and translocation of signal transducers and activators of transcription 1 (STAT1), neuronal immunoreactivity to interferon regulatory factor 1 (IRF-1), and activation of OAS occur in models of cerebral ischemia and in neurons subjected to ischemic stress [36–38]. Alternatively, in light of the role of RNase-L in apoptosis IFN [26,29,39,40], RNase-L activity could modulate a step upstream of mt-mRNA decay rather than directly modulating the effect. Ribosomal RNA and viral RNAs have been first described as targets of RNase-L [21]. Recently, cellular mRNAs have been described as targets of RNase-L. These include interferon-regulated genes 43 and 15 mRNAs, and myoD mRNA [41,42]. This study extends these results to suggest that RNase-L also regulates the stability of mitochondrial mRNAs. Regulation of mt-mRNA expression by RNase-L may explain how RNase-L could play a role in pro-apoptotic and growth inhibitory activities.

Acknowledgment

This work was supported by the grants from NIH NS045081 (K.C.), AHA 0256383U (K.C.), and US Army DAMD17-99-1-9483.

References

- [1] G. Attardi, G. Schatz, *Annu. Rev. Cell Biol.* 4 (1988) 289–333.
- [2] L.A. Grivell, *Eur. J. Biochem.* 182 (1989) 477–493.
- [3] R.J. Wiesner, T.T. Kurowski, R. Zak, *Mol. Endocrinol.* 6 (1992) 1458–1467.
- [4] R.J. Wiesner, T.V. Hornung, J.D. Garman, D.A. Clayton, E. O’Gorman, T. Wallimann, *J. Bioenerg. Biomembr.* 31 (1999) 559–567.
- [5] C. Zhang, M.T. Wong-Riley, *J. Neurosci. Res.* 60 (2000) 338–344.
- [6] G. Gaines, C. Rossi, G. Attardi, *J. Biol. Chem.* 262 (1987) 1907–1915.
- [7] J.A. Enriquez, P. Fernandez-Silva, A. Perez-Martos, M.J. Lopez-Perez, J. Montoya, *Eur. J. Biochem.* 237 (1996) 601–610.
- [8] S.F. DasGupta, S.I. Rapoport, M. Gerschenson, E. Murphy, G. Fiskum, S.J. Russell, K. Chandrasekaran, *Mol. Cell Biochem.* 221 (2001) 3–10.
- [9] K. Chandrasekaran, L.I. Liu, K. Hatanpaa, U. Shetty, Z. Mehrabian, P.D. Murray, G. Fiskum, S.I. Rapoport, *Mitochondrion* 1 (2001) 141–150.
- [10] A.B. Sachs, *Cell* 74 (1993) 413–421.
- [11] J. Ross, *Microbiol. Rev.* 59 (1995) 423–450.
- [12] C.M. Brennan, J.A. Steitz, *Cell Mol. Life Sci.* 58 (2001) 266–277.
- [13] J. Guhaniyogi, G. Brewer, *Gene* 265 (2001) 11–23.
- [14] G. Attardi, A. Chomyn, M.P. King, B. Kruse, P.L. Polosa, N.N. Murdter, *Biochem. Soc. Trans.* 18 (1990) 509–513.
- [15] N.G. Avadhani, *Biochemistry* 18 (1979) 2673–2678.
- [16] D.E. Buetow, W.M. Wood, *Subcell. Biochem.* 5 (1978) 1–85.
- [17] G. Attardi, J. Montoya, *Methods Enzymol.* 97 (1983) 435–469.
- [18] K. Grohmann, F. Amairic, S. Crews, G. Attardi, *Nucleic Acids Res.* 5 (1978) 637–651.
- [19] F. Le Roy, C. Bisbal, M. Silhol, C. Martinand, B. Lebleu, T. Salehzada, *J. Biol. Chem.* 276 (2001) 48473–48482.
- [20] J.A. Lewis, A. Huq, P. Najarro, *J. Biol. Chem.* 271 (1996) 13184–13190.
- [21] G.R. Stark, I.M. Kerr, B.R. Williams, R.H. Silverman, R.D. Schreiber, *Annu. Rev. Biochem.* 67 (1998) 227–264.
- [22] R.H. Silverman, in: J. Belasco, G. Brawerman (Eds.), *Ribonucleases Structure and Functions*, Academic Press, New York, 1997, pp. 515–551.
- [23] B. Dong, R.H. Silverman, *J. Biol. Chem.* 272 (1997) 22236–22242.
- [24] J.C. Castelli, B.A. Hassel, K.A. Wood, X.L. Li, K. Amemiya, M.C. Dalakas, P.F. Torrence, R.J. Youle, *J. Exp. Med.* 186 (1997) 967–972.
- [25] M. Diaz-Guerra, C. Rivas, M. Esteban, *Virology* 236 (1997) 354–363.
- [26] J.C. Castelli, B.A. Hassel, A. Maran, J. Paranjape, J.A. Hewitt, X.L. Li, Y.T. Hsu, R.H. Silverman, R.J. Youle, *Cell Death Differ.* 5 (1998) 313–320.
- [27] A. Zhou, J.M. Paranjape, B.A. Hassel, H. Nie, S. Shah, B. Galinski, R.H. Silverman, *J. Interferon Cytokine Res.* 18 (1998) 953–961.
- [28] G.N. Barber, *Cell Death Differ.* 8 (2001) 113–126.
- [29] A. Zhou, J. Paranjape, T.L. Brown, H. Nie, S. Naik, B. Dong, A. Chang, B. Trapp, R. Fairchild, C. Colmenares, R.H. Silverman, *EMBO J.* 16 (1997) 6355–6363.
- [30] K. Chandrasekaran, T. Giordano, D.R. Brady, J. Stoll, L.J. Martin, S.I. Rapoport, *Brain Res. Mol. Brain Res.* 24 (1994) 336–340.
- [31] R. Gelfand, G. Attardi, *Mol. Cell. Biol.* 1 (1981) 497–511.
- [32] G.C. Sen, P. Lengyel, *J. Biol. Chem.* 267 (1992) 5017–5020.
- [33] T. Salehzada, M. Silhol, B. Lebleu, C. Bisbal, *J. Biol. Chem.* 266 (1991) 5808–5813.
- [34] S. Besse, D. Rebouillat, I. Marie, F. Puvion-Dutilleul, A.G. Hovanessian, *Exp. Cell Res.* 239 (1998) 379–392.
- [35] P.G. Young, G. Attardi, *Biochem. Biophys. Res. Commun.* 65 (1975) 1201–1207.
- [36] W. Paschen, S. Althausen, J. Douthail, *Neurosci. Lett.* 263 (1999) 109–112.
- [37] Y. Takagi, J. Harada, A. Chiarugi, M.A. Moskowitz, *J. Cereb. Blood Flow Metab.* 22 (2002) 1311–1318.
- [38] M. Alexander, C. Forster, K. Sugimoto, H.B. Clark, S. Vogel, M.E. Ross, C. Iadecola, *Acta Neuropathol. (Berl)* 105 (2003) 420–424.
- [39] B.A. Hassel, A. Zhou, C. Sotomayor, A. Maran, R.H. Silverman, *EMBO J.* 12 (1993) 3297–3304.
- [40] G. Li, Y. Xiang, K. Sabapathy, R.H. Silverman, *J. Biol. Chem.* 279 (2004) 1123–1131.
- [41] X.L. Li, J.A. Blackford, C.S. Judge, M. Liu, W. Xiao, D.V. Kalvakolanu, B.A. Hassel, *J. Biol. Chem.* 275 (2000) 8880–8888.
- [42] C. Bisbal, M. Silhol, H. Laubenthal, T. Kaluza, G. Carnac, L. Milligan, F. Le Roy, T. Salehzada, *Mol. Cell. Biol.* 20 (2000) 4959–4969.